

# An Integrated Driver for the Electrical Stimulation of the Optic Nerve

Pascal Doguet<sup>°</sup>, Hervé Mevel<sup>°</sup>, Michel Verleysen<sup>°</sup>, Michel Troosters<sup>°°</sup>, Charles Trullemans<sup>°</sup>

<sup>°</sup> Microelectronics Laboratory,  
Université catholique de Louvain  
Place du Levant, 3  
B-1348, Louvain-la-Neuve, Belgium  
E-mail: c.trullemans@dice.ucl.ac.be

<sup>°°</sup> Neurotech S.A.  
Place des Peintres, 7  
B-1348, Louvain-la-Neuve, Belgium

**Abstract** – *The integrated driver is part of a specific integrated circuit meant to be encapsulated within an implanted neural stimulator. Current waveform specifications are derived from the requirements of a visual prosthesis by stimulation of the optic nerve. The driver features small current steps (1  $\mu$ A), large current (-6 to +6 mA) and voltage (-12 to +12V) swings, fast settling time (2  $\mu$ s) and automatic active charge recovery. Internal driver schematic and data measured on system samples are given.*

**Keywords:** Neural stimulation, implanted stimulator, visual prosthesis, charge recovery.

## 1. Introduction

The electrical stimulation of the optic nerve has been investigated as an approach to the development of a microsystem based visual prosthesis [1].

The integrated driver described here is part of a specific integrated circuit (fig. 1) that is meant to be encapsulated and implanted in the final, autonomous version of the prosthesis (patent pending).

The integrated circuit contains the interface to a transcutaneous link (carrier frequency: 12 MHz, incoming data rate 3 Mbit/sec, back channel bursts at 3 Mbit/s), the power supplies, a logic bloc handling the transmission protocol and the driver control, and the integrated driver.

External commands can be transmitted through the incoming link to modify the parameters of the current sources, to control the charge recovery, or to ask for electrode or internal voltages measurements. Transmission protocol data and 8-bit values can be sent out by the back channel. This allows the monitoring of the electrode impedance.

The integrated circuit contains four independent drivers; four circuits can be associated to drive a total number of 16 electrodes from a single transcutaneous link.

## 2. Driver specifications

The driver is basically a current source, producing an arbitrary current waveform described as a staircase (fig.2)

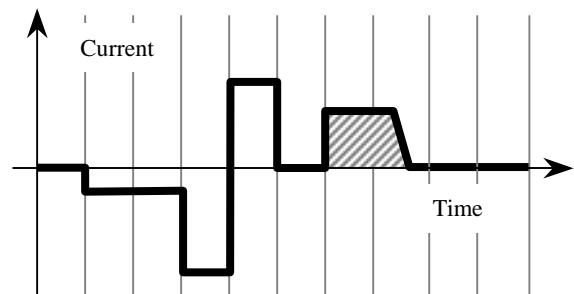


Fig. 2: Typical staircase current waveform; the hatched pulse results from the automatic charge recovery.

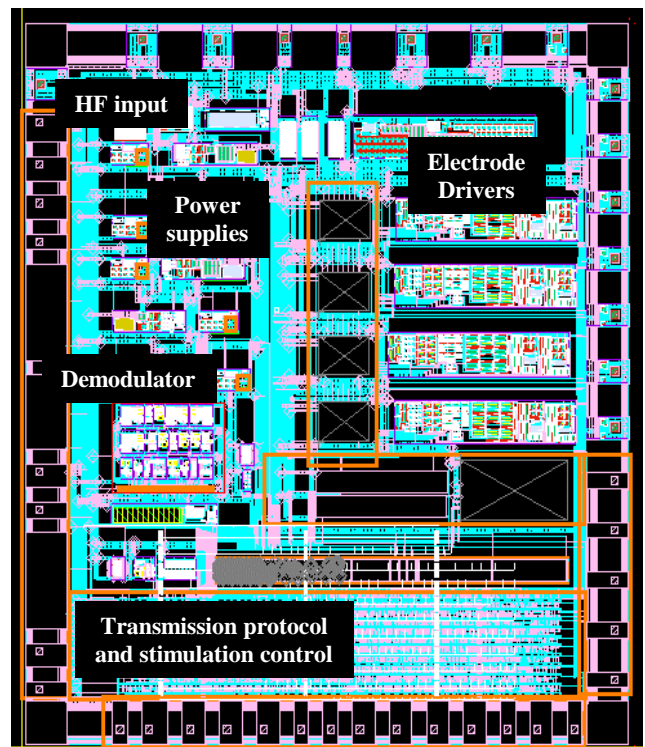


Fig.1: Layout of the integrated

from digital data and commands transmitted through a

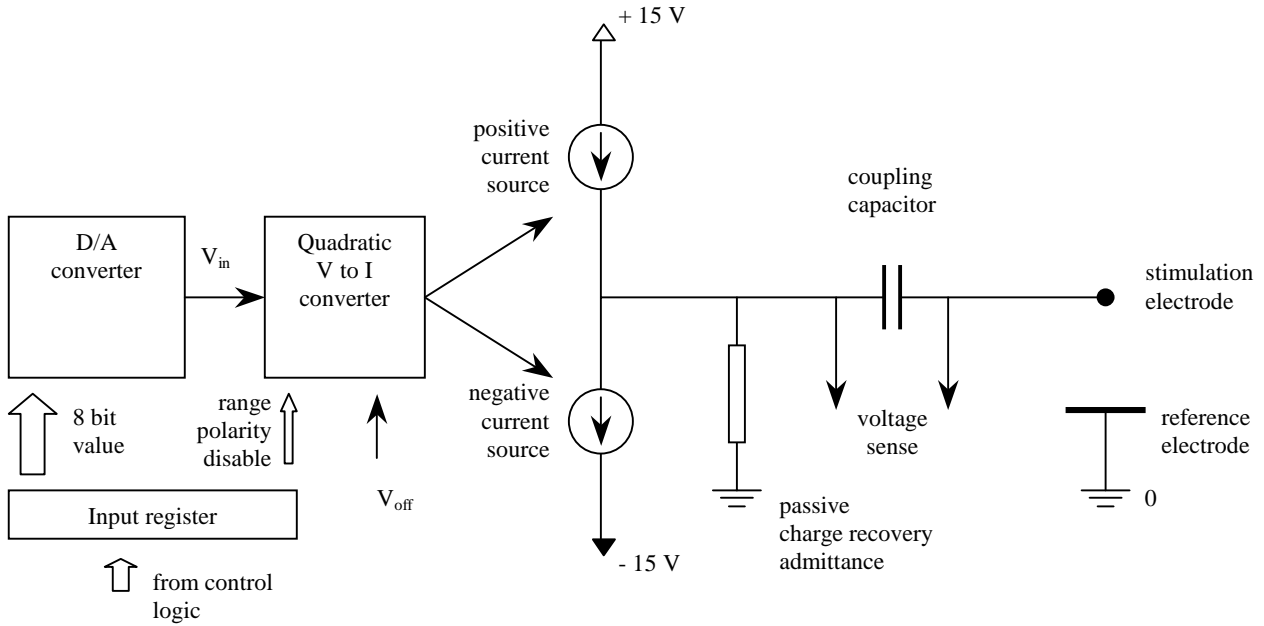


Fig. 3: Driver functional diagram

current range, high :	from -6 mA to +6mA
current range, low :	from -490 $\mu$ A to 490 $\mu$ A
current step size:	10% of the current magnitude from 10 $\mu$ A
minimal current step:	1 $\mu$ A
current step range:	from 1 to 600 $\mu$ A
precision of the current :	
uncalibrated:	10%,
calibrated:	better than 2%
time step :	21.3 $\mu$ s
settling time:	shorter than 2 $\mu$ s
load impedance:	500 to 2000 ohms
output impedance	higher than 100 kohms
voltage swing:	-12 to +12 V

Table 1: Specifications of the current driver

transcutaneous link. The time step, related to the transcutaneous link carrier period from which the main clock is derived, is about 20 microseconds.

A visual prosthesis asks for continuous stimulations during a long period, at a high stimulation rate. Therefore, the need for canceling quickly any unwanted charge building up at the electrode [2] asks for a careful design of the charge recovery scheme. The designed automatic scheme is described in section 4. The hatched pulse showed on fig. 2 results from a recovery command sent through the link.

According to the classical scheme, the current source drives the electrode through an external series capacitor (fig. 3); voltage sensing across the coupling capacitor allows the monitoring of the electrode voltage and of the total charge integrated by the capacitor itself. This charge is a measure of the net charge injection into the electrode.

Table 1 summarizes the driver specifications.

### 3. Driver structure

The overall structure of the driver is described by the figure 3. Figure 4 gives a detailed schematic of the main parts.

The output current magnitude is fed as an 8-bit logical word to the driver input register. This register is loaded at the master clock edge whenever a command asking to update the magnitude is received; a sequence of such commands describes a staircase waveform (fig. 2). Additional bits control the current range, the output polarity and the disabled condition, where the output driver is switched off regardless of the magnitude stored in the register. A reference voltage,  $V_{off}$ , sets the lower end of the current ranges; this reference voltage is set by a bandgap reference at 1.2V.

A simple 8-bit converter performs the conversion from the digital data to an analog voltage. A converter cell able to meet the precision and speed specifications while minimizing the power drain was indeed available as a proven library cell.

From the converter output, the driver is made up from three main stages (fig. 4): the first one is a voltage to current quadratic converter; the second one handles the range, polarity and disable controls; the third stage is the bipolar current output source.

The voltage to current converter provides a reference current from the D/A converter analog output voltage.

The precision requirement is not expressed as an absolute precision, but as a precision relative to the current magnitude; therefore an exponential converter should be an

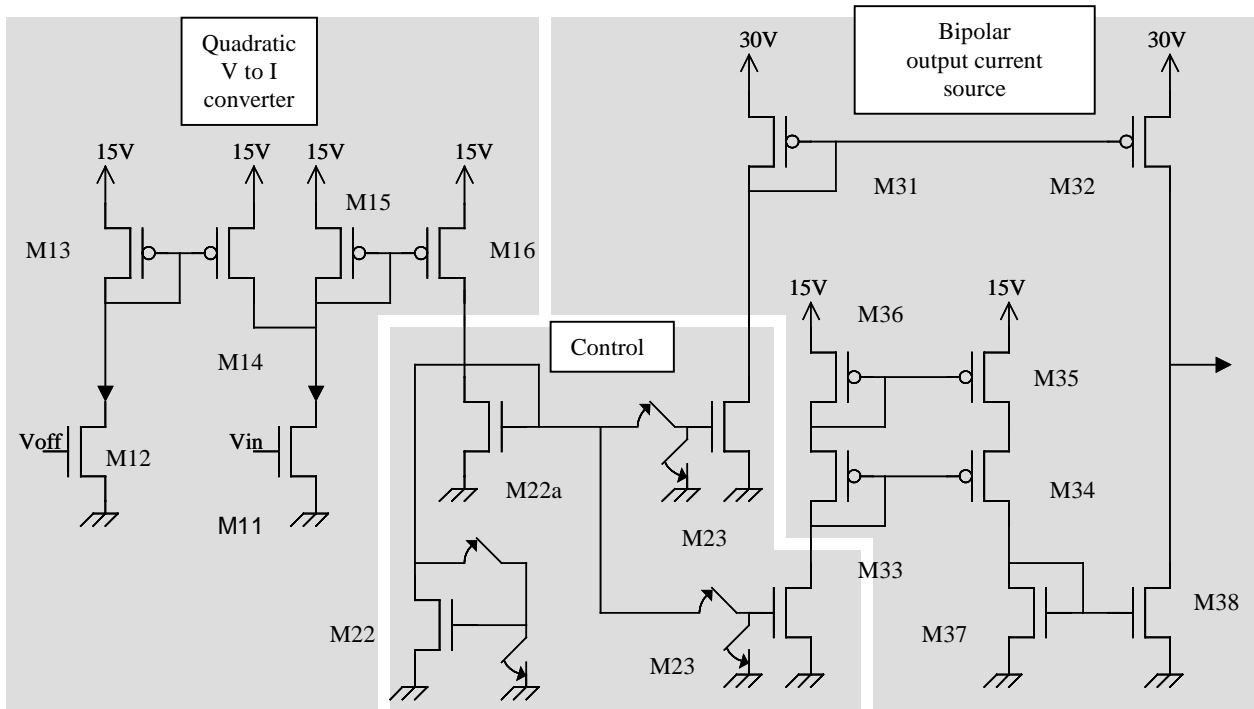


Fig. 4: Current driver schematic

ideal solution. However, the natural quadratic law of a MOS transistor transadmittance can provide the necessary swing and resolution. An advantage of the MOS transistor is that its gate may be directly driven between 0 to 5V by the output of the D/A converter; hence the complexity of the resulting circuit is kept low.

The analog input voltage  $V_{in}$  sets the output reference current by controlling M11. The temperature dependence of this current is limited to less than 10% within a temperature range of 20 °C thanks to a differential offset compensation stage made up from the transistors M11 and M12. The drain current of M12, controlled by the biasing voltage  $V_{off}$ , is mirrored by M13 and M14 and subtracted from the drain current of M11. The current difference is mirrored by M15 and M16; M16 delivers the reference current to the next stage.

The reference current is obviously zero when  $V_{in}=V_{off}$ .  $V_{off}$  is thus a threshold voltage defining the actual lower end of the current ranges.

The simple circuit used for the previous stage cannot fulfill the compromise between the need for a high absolute precision for small stimulation currents and the need for a large current swing. However, the external processor

controlling the whole system stores a calibration table. Two separate current ranges can thus be conveniently defined.

A control bit switches between a low range (0 to 490  $\mu$ A, smaller step 1  $\mu$ A) and a high range (0 to 6 mA, smaller step 24  $\mu$ A). This bit controls the gain of the mirror M21a/M22b-M23p/M23n, by turning M22a on or off.

The polarity control bit switches the output current through M23p to the positive output, or through M23n to the negative output.

The disable control bit switches M23p and M23n off simultaneously. As a result, a secure zero current output may be quickly achieved and guaranteed by a single command, without any concern for the analog value of the reference voltage at the input of the converter.

A careful sizing of the switching transistors is required to keep the effect of the parasitic charges injected from the switch gates negligible.

The positive output source is a simple current mirror M31-M32. The mirror M33 to M34 reverses the polarity of the current and drives the negative output source M37-M38.

#### 4. Charge recovery

A classical solution to the charge recovery specification is to apply (1) active recovery, by computing the waveform parameters in order to balance the integrated charge and (2) passive recovery, by sinking any residual charges through an integrated small admittance (see fig. 3).

A passive recovery is necessary because of the discrete

```

when a recovery command is received
  for one time step
    switch positive and negative source off
    StartPolarity <- CouplingCapPolarity
  endfor
  while (CouplingCapPolarity==StartPolarity)
    if (StartPolarity) switch negative source on
    else switch positive source on
    endif
  endwhile
  switch positive and negative source off
endwhen

```

Table 2: Automatic active charge recovery algorithm

nature of the current magnitude and of the time step, and because the finite precision of the current sources defeats the active recovery scheme. Furthermore, if the residual charge is too big, either the current peak implied by the passive recovery is too large, either the recuperation is too slow.

These drawbacks cannot be afforded in the case of the visual prosthesis. Hence an automatic active charge recovery scheme controlled by a feedback loop has been implemented.

The feedback ensures that the recovery is fairly completed by the active scheme under local analog control. The local control is implemented as an asynchronous circuit working in continuous time, i.e. without error due to discrete time steps.

A sign detector connected to the voltage sensing terminals across the coupling capacitor (fig.3) provides the logical signal CouplingCapPolarity.

The magnitude of the current used during the recuperation is a parameter that can be set at any time by a command sent through the transcutaneous link. When a recovery command is sent in the same way, the recuperation algorithm described by Table 2 is applied. The charge is removed by the current source until a polarity change is detected. At this time, the voltage across the capacitor is equal to the comparator offset. The effect of the system is to bring the coupling capacitor back to the same voltage after every recovery command. This process cancels the net charge integrated between two recovery commands.

Some charge is however integrated during the propagation delay through the comparator, the asynchronous control logic and the current sources. This results in a small residual charge, proportional to the recovery current, that can be conveniently handled by the passive recovery

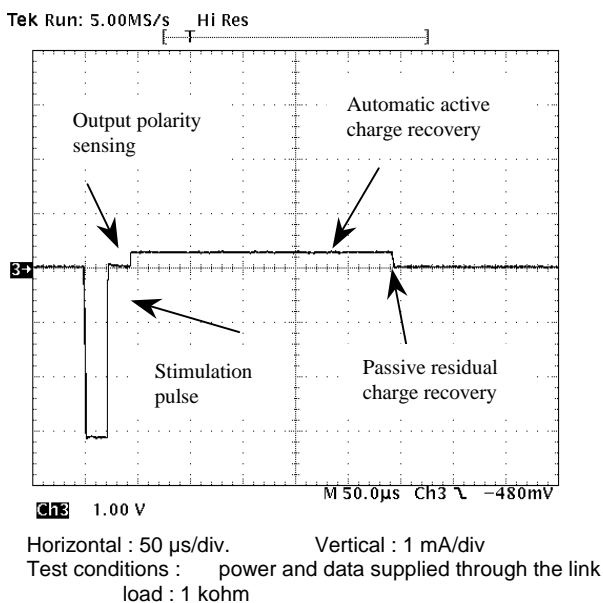


Fig. 6: Measured stimulation pulse

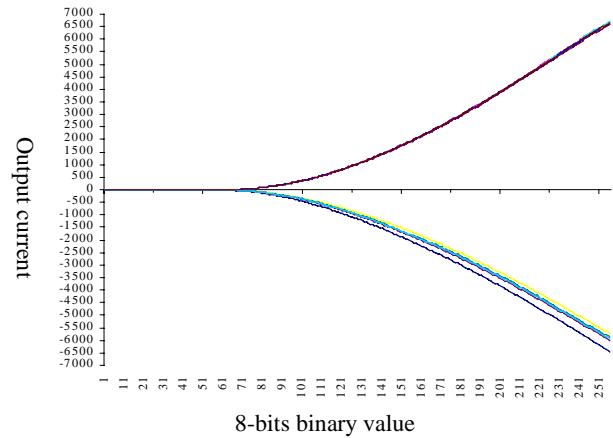


Fig. 5: Measured output current vs input binary value for several circuit samples (high range)

admittance.

## 5. Results

The circuit has been processed and characterized. The Mietec I2T technology has been chosen because of the system voltage requirements.

The quadratic converter transfer function is illustrated by fig. 5 for both polarities. Negative currents exhibit 7% amplitude dispersion between different circuit samples. This is related to technological reasons, but can be easily compensated during calibration.

Figure 6 illustrates the behavior of the recovery scheme. After the negative pulse (- 3 mA), a dead period is introduced for polarity measurement. Automatic recovery is performed at a 250 µA positive current. The passive recovery is barely visible, attesting for a negligible residual charge.

The realized integrated drivers comply with all the specifications given in table 2.

The implantable stimulator, designed to meet the difficult requirements specified in the frame of a visual prosthesis, is suitable for wide application areas.

## References

[1] Veraart C., Delbeke J., Wanet-Defalque M.-C., Vanlierde A., Michaux G., Parrini S., Glineur O., Verleysen M., Trullemans C., and Mortimer J.T. (1999) *Selective stimulation of the human optic nerve*. Proceedings of the 4th Conference of the International Functional Electrical Stimulation Society, Sendai, Japan, August 23-27, : 57-59.

see also : <http://www.dice.ucl.ac.be/mivip>

[2] N. de N. Donaldson and P.E.K. Donaldson,

(1986) *When are actively balanced biphasic stimulating pulses necessary in neurological prosthesis ?* Medical & Biomedical Engineering & Computing, pp. 41-49, January 1986. .

## Acknowledgments

This work has been performed in the frame of the ESPRIT LTR project MIVIP under a grant from the European commission.